Fractional protein dynamics seen by nuclear magnetic resonance spectroscopy: Relating molecular dynamics simulation and experiment

Vania Calandrini,[1,2,a)] Daniel Abergel,[3,b)] and Gerald R. Kneller[1,2,4,c)]
[1]*Centre de Biophysique Moléculaire, CNRS, Rue Charles Sadron, 45071 Orléans, France*
[2]*Synchrotron Soleil, L'Orme de Merisiers, B.P. 48, 91192 Gif-sur-Yvette, France*
[3]*Département de Chimie, UMR 7203 CNRS et Université Pierre et Marie Curie, Ecole Normale Supérieure, 24 rue Lhomond, 75231 Paris Cedex 05, France*
[4]*Université d'Orléans, Chateau de la Source-Av. du Parc Floral, 45067 Orléans, France*

(Received 23 April 2010; accepted 13 August 2010; published online 11 October 2010)

We propose a fractional Brownian dynamics model for time correlation functions characterizing the internal dynamics of proteins probed by NMR relaxation spectroscopy. The time correlation functions are represented by a broad distribution of exponential functions which are characterized by two parameters. We show that the model describes well the restricted rotational motion of N–H vectors in the amide groups of lysozyme obtained from molecular dynamics simulation and that reliable predictions of experimental relaxation rates can be obtained on that basis. © *2010 American Institute of Physics*. [doi:10.1063/1.3486195]

I. INTRODUCTION

NMR relaxation spectroscopy has proven to be a unique approach for a site-specific investigation of both global tumbling and internal motions of proteins. The molecular motions modulate the magnetic interactions between the nuclear spins and lead for each nuclear spin to a relaxation behavior which reflects its environment. Since its first applications to the study of protein dynamics, a variety of techniques has been proposed for the investigation of both backbone and side chain dynamics. Among them, relaxation measurements of backbone amide ^{15}N nuclei, which are routinely studied by NMR, are most widespread.

The relationship between microscopic motions and spin relaxation rates is provided by Redfield's theory.[1] In the case of backbone amide ^{15}N, relaxation primarily occurs through fluctuations of the ^{15}N–^{1}H-dipole-dipole interactions with the directly bonded amide proton and of the ^{15}N chemical shift anisotropy tensor, which is commonly assumed to be axially symmetric with its axis parallel to the NH bond (for a general reference, see Ref. 2). The relaxation rates of the ^{15}N nuclei are determined by time correlation functions (TCFs) of the form

$$C_{ii}(t) = \langle P_2(\boldsymbol{\mu}_i(t) \cdot \boldsymbol{\mu}_i(0)) \rangle, \tag{1}$$

where $\boldsymbol{\mu}_i(t)$ is a unit vector pointing along the NH bond of residue i and $P_2(.)$ is the second order Legendre polynomial. Longitudinal and transverse ^{15}N relaxation rates (R_{1i} and R_{2i}), and ^{15}N{^{1}H} heteronuclear Overhauser enhancement ($\eta_{\mathrm{NH}i}$) are expressed as linear combinations of the spectral density functions $J_{ii}(\omega)$, the Fourier transforms of the $C_{ii}(t)$, which are evaluated at the Larmor frequencies 0, ω_{H}, ω_{N}, and $\omega_{\mathrm{H}\pm\mathrm{N}} \equiv \omega_{\mathrm{H}} \pm \omega_{\mathrm{N}}$

$$\eta_{\mathrm{NH}i} = 1 + \frac{\gamma_{\mathrm{H}}}{\gamma_{\mathrm{N}}} \frac{d^2}{R_1} (6J_{ii}(\omega_{\mathrm{H+N}}) - J_{ii}(\omega_{\mathrm{H-N}})), \tag{2a}$$

$$R_{1i} = d^2(3J_{ii}(\omega_{\mathrm{N}}) + J_{ii}(\omega_{\mathrm{H-N}}) + 6J_{ii}(\omega_{\mathrm{H+N}})) + 2c^2 J_{ii}(\omega_{\mathrm{N}}), \tag{2b}$$

$$R_{2i} = d^2\left(2J_{ii}(0) + \frac{3}{2}J_{ii}(\omega_{\mathrm{N}}) + \frac{1}{2}J_{ii}(\omega_{\mathrm{H-N}}) + 3J_{ii}(\omega_{\mathrm{H}}) + 3J_{ii}(\omega_{\mathrm{H+N}})\right) + c^2\left(\frac{4}{3}J_{ii}(0) + J_{ii}(\omega_{\mathrm{N}})\right). \tag{2c}$$

Here $d = \mu_0 \hbar \gamma_{\mathrm{H}} \gamma_{\mathrm{N}} / 4\sqrt{10}\pi \langle r_{\mathrm{NH}}^3 \rangle$ and $c = \gamma_{\mathrm{N}} B_0 \Delta\sigma_{\mathrm{N}} / \sqrt{15}$. The parameters γ_{H} and γ_{N} are the gyromagnetic ratios of ^{15}N and ^{1}H atoms, respectively, μ_0 is the vacuum magnetic susceptibility, $\hbar$ is the reduced Planck constant, and $\Delta\sigma_{\mathrm{N}}$ is the ^{15}N chemical shift anisotropy. The NH distance is considered constant and is fixed to its average value $\langle r_{\mathrm{NH}} \rangle$.

The Redfield equations show that relaxation measurements probe the relaxation dynamics of a selected nuclear spin at only five selected frequencies. It is therefore not possible in practice to obtain a detailed picture about the internal and global dynamics of proteins by a numerical reconstruction of $J_{ii}(\omega)$ from NMR data. In the model-free (MF) approach by Lipari and Szabo[3] the assumption is made that the internal reorientational correlation function decays exponentially. Various studies of protein dynamics, spanning time scales from picoseconds to hours[4–10] give, however, evidence that internal protein dynamics is characterized by strongly nonexponential TCFs which may be described by non-Markovian stochastic models, such as fractional Brownian dynamics (fBD) and the continuous time random walk (CTRW).[11] The TCFs resulting from such models are characterized by a superposition of exponential functions, with a broad spectrum of decay rates. In the context of NMR spectroscopy we have recently shown[12] that these relaxation

a)Electronic mail: vania.calandrini@cnrs-orleans.fr.
b)Electronic mail: daniel.abergel@ens.fr.
c)Electronic mail: gerald.kneller@cnrs-orleans.fr.

spectra are compatible with those found from elastic network models for the interpretation of NMR relaxation data.[13,14]

In this article we demonstrate that fBD is also a good basis to describe the rotational diffusion of NH bond vectors resulting from the internal dynamics of proteins seen in molecular dynamics (MD) simulations, and that reliable estimations for experimental NMR relaxation rates can be obtained on that basis. The physical motivation is discussed and an illustrative example is presented for the case of lysozyme, where the predicted NMR relaxation rates obtained from fits of the corresponding MD correlation functions are compared to experimental.[15]

II. MD SIMULATION

A. Simulation protocol

The simulated system consists of one hen egg white lysozyme molecule and 6775 water molecules. As starting configuration of the protein we used the crystallographic structure corresponding to entry 193L of the Brookhaven Protein Data Bank.[16] The hydrogen atoms of the protein were added according to standard criteria for the chemical bond structure of amino acids, leading to a system of 22295 atoms in total. The simulation has been performed with the program package NAMD,[17] using the AMBER99SB (Ref. 18) and Simple Point Charge-Extended (SPC/E) (Ref. 19) force fields for the protein and the water molecules, respectively. To mimic a macroscopic system, periodic boundary conditions have been applied and electrostatic interactions have been computed using the particle mesh Ewald method,[20] with a cutoff of 12 Å. The integration time step was set to 1 fs and atomic configurations were recorded with a sampling time step of 50 fs over 10 ns in total. The simulation has been carried out at ambient conditions, using a Langevin thermostat[21] and a Nose–Hoover barostat.[22] In order to extract a trajectory describing only the internal dynamics of the simulated lysozyme molecule, global translations and rotations of the protein molecule have been filtered out by performing for each sampling time step a rigid body fit of its actual conformation to its initial conformation in the trajectory.[23,24]

B. Calculation of rotational correlation functions

Assuming that the overall tumbling motion is isotropic and statistically uncorrelated with the internal motions, the total correlation function can be factorized as

$$C_{ii}(t) = C^G(t)C^I_{ii}(t), \tag{3}$$

where $C^G(t)$ and $C^I_{ii}(t)$ are the global and internal correlation function, respectively.[3] This factorization does not require the internal correlation function to relax much faster than the global one.[25] Such an assumption would be incompatible with fBD, which implies the presence of arbitrarily long time relaxation times. It is sufficient to assume that the global and internal motions are statistically independent (for a recent and detailed discussion, see Ref. 26). To compute the internal TCFs from the simulated trajectory we used the representation

$$C^I_{ii}(t) = \frac{4\pi}{5}\sum_{m=-2}^{2}(-1)^m\langle Y_2^{-m}(\Omega_i(0))Y_2^m(\Omega_i(t))\rangle, \tag{4}$$

which allows for an efficient calculation by fast Fourier transform techniques.[27] Here, Ω_i denotes the polar angles defining the instantaneous orientation of the ith NH vector in the molecular reference frame, and $Y_2^m(\cdot)$ is the second rank spherical harmonic.[28] The asymptotic values were computed through

$$S_i^2 = \lim_{t\to\infty} C^I_{ii}(t) = \frac{4\pi}{5}\sum_{m=-2}^{2}|\langle Y_2^m(\Omega_i)\rangle|^2. \tag{5}$$

III. THEORY

A. Model for internal correlation functions

In absence of detailed information on the rotational diffusion of NH vectors, it is natural to assume an exponential decay of the corresponding autocorrelation function. As mentioned above, this approach is used in the MF analysis of Lipari and Szabo.[3] It implies in particular the assumption of one dominant relaxation process, with an associated relaxation rate. It will be shown later that the TCFs relevant to NMR relaxation display, however, a strongly nonexponential form—in agreement with the observations from other spectroscopic experiments cited above. To account for multiple relaxation processes with a broad spectrum of relaxation rates, we assume the following model for the internal TCFs:

$$C^I_{ii}(t) = S_i^2 + (1 - S_i^2)E_{\alpha_i}(-[t/\tau_i]^{\alpha_i}). \tag{6}$$

Here $E_\alpha(\cdot)$ is the Mittag–Leffler (ML) function

$$E_\alpha(z) = \sum_{k=0}^{\infty}\frac{z^k}{\Gamma(1+\alpha k)} \tag{7}$$

which is an entire function in the domain of complex numbers[29] and the parameter α is in general complex. The asymptotic value $S_i^2 = C^I_{ii}(\infty)$ is the so-called generalized order parameter[3] which indicates the degree of spatial restriction of the internal motions of a bond vector, and the parameter τ_i sets the time scale of the internal relaxation processes.

The function $E_\alpha(-[t/\tau]^\alpha)$ in Eq. (6) can be viewed as a generalization of a stretched exponential function with α and τ being the shape and scale parameters, respectively. For $\alpha=1$ the stretched ML function reduces to an exponential function, whereas it exhibits a power law decay at large times for $0<\alpha<1$, $E_\alpha(-[t/\tau]^\alpha)\propto(t/\tau)^{-\alpha}$, and an infinitely steep decay at $t=0$. The MF approach of Lipari and Szabo thus appears as a special case of Eq. (6), by setting $\alpha=1$. The deviation of the stretched ML function from the exponential law can be described in terms of a distribution function $p_{\alpha,\tau}(\lambda)$ for the relaxation rates λ

$$E_\alpha(-[t/\tau]^\alpha) = \int_0^\infty d\lambda p_{\alpha,\tau}(\lambda)\exp(-\lambda t). \tag{8}$$

The relaxation spectrum is positive and has the form[4,7]

$$p_{\alpha,\tau}(\lambda) = \frac{\tau}{\pi}\frac{(\tau\lambda)^{\alpha-1}\sin(\pi\alpha)}{(\tau\lambda)^{2\alpha} + 2(\tau\lambda)^{\alpha}\cos(\pi\alpha) + 1}, \tag{9}$$

where $0<\alpha\leq 1$. It verifies the normalization condition $\int_0^\infty d\lambda p_{\alpha,\tau}(\lambda)=1$ and for $\alpha=1$ it reduces to a Dirac distribution centered at $\lambda=\tau^{-1}$. The inverse of the scaling parameter τ gives the median of $p_{\alpha,\tau}(\lambda)$.[9] For $0<\alpha<1$ the stretched ML function exhibits self-similarity on the time scale and is the solution of a fractional differential equation.[4,30] We thus propose a self-similar, fractional extension of the MF approach. The interpretation in terms of a dynamical model represents a further step in the analysis, on which we comment below.

B. Physical interpretation

Correlation functions of the form $E_\alpha(-[t/\tau]^\alpha)$ arise in the context of a certain class of so-called anomalous diffusion processes, which are observed in a variety of complex systems.[31] In case of one-dimensional free diffusion, the anomaly refers to a sublinear evolution of the mean-square displacement in time, $\langle[x(t)-x(0)]^2\rangle=2D_\alpha t^\alpha(0<\alpha<1)$, where D_α is the fractional diffusion constant. The spatial restriction of atomic motions in proteins can be accounted for by the Ornstein–Uhlenbeck (OU) process,[32–35] which describes the diffusion of a particle in a harmonic potential. In the context of protein dynamics the harmonic potential must be viewed as an effective potential, describing the "softness" or "resilience" of a protein.[36] The standard OU process leads, however, to an exponentially decaying autocorrelation function for the dynamical variable, in contrast to what is observed in the experiments and simulations. These observations can be accounted for by using instead the fractional OU (fOU) process to describe intramolecular motions,[11] which exhibits non-Markovian long time memory effects.[6,37] Alternatively, the latter can be thought of as a CTRW on a "rugged" parabolic energy surface, with a broad distribution of the waiting times between successive displacements.[11] This approach has been used in the various experimental and simulation studies of internal protein dynamics mentioned above, considering as dynamical variables atomic position fluctuations,[7–10] fluctuations of position differences,[5] and Fourier-transformed particle densities.[6] A relation between fractional Brownian dynamics and rugged potential energy surfaces can be established by mapping the average waiting times or relaxation rates onto barrier heights separating the various conformational "substates" in the protein potential energy surface.[4,38] In this kinetic description of protein dynamics one can think of a "fractal" potential energy surface,[39] which corresponds to "fractional" Brownian dynamics.

In the simplest case of a one-dimensional (1D) random diffusion process, the probability density associated with the fOU process is the solution of a fractional Fokker–Planck equation

$$\frac{\partial P(x,t|x_0,0)}{\partial t} = \tilde{\tau}^{1-\alpha}\,{}_0\mathcal{D}_t^{1-\alpha}\mathcal{L}P(x,t|x_0,0), \tag{10}$$

where $\mathcal{L}$ is the usual Fokker–Planck operator acting on the relevant dynamical variable x. For simplicity we consider for the moment a 1D stochastic process. The symbol ${}_0\mathcal{D}_t^{1-\alpha}$ defines a fractional derivative of order $1-\alpha$, which is defined through[40]

$${}_0\mathcal{D}_t^{1-\alpha}f(t) = \frac{d}{dt}\int_0^t d\tau\frac{(t-\tau)^{\alpha-1}}{\Gamma(\alpha)}f(\tau), \quad 0<\alpha\leq 1, \tag{11}$$

where $\Gamma(\cdot)$ is the generalized factorial.[28] The factor $\tilde{\tau}^{1-\alpha}$, where $\tilde{\tau}$ has the dimension of time, ensures the correct dimension of the right-hand side of Eq. (10). In the case of an fOU process $\mathcal{L}$ is of Smoluchowski type

$$\mathcal{L} = D\frac{\partial}{\partial x}\left\{\frac{1}{k_BT}\frac{\partial V(x)}{\partial x} + \frac{\partial}{\partial x}\right\}, \tag{12}$$

where D is the diffusion constant of free diffusion,

$$V(x) = Kx^2/2 \tag{13}$$

is the potential in which the particle moves, and k_B and T denote, respectively, the Boltzmann constant and the absolute temperature.

Since $\mathcal{L}$ has a discrete spectrum of eigenvalues, the solution of Eq. (10) can be developed in terms of its left and right eigenfunctions, following exactly the same procedure as for the normal OU process.[33,35] In terms of the dimensionless variable $\xi=x/\sqrt{x^2}$, where

$$\langle x^2\rangle = \frac{k_BT}{K} \tag{14}$$

is the mean square position fluctuation, one finds the following form for the transition probability density:[11]

$$P(\xi,t|\xi_0,0) = \frac{\exp\left(-\frac{\xi^2}{2}\right)}{\sqrt{2\pi}}\sum_{n=0}^{\infty}\frac{1}{2^n n!}H_n\left(\frac{\xi}{\sqrt{2}}\right)H_n\left(\frac{\xi_0}{\sqrt{2}}\right) \times E_\alpha(-n\eta_\alpha t^\alpha). \tag{15}$$

The functions H_n are Hermite polynomials[28] and η_α is the fractional relaxation rate

$$\eta_\alpha = \frac{D\tilde{\tau}^{1-\alpha}}{\langle x^2\rangle}. \tag{16}$$

The knowledge of the transition probability density P permits to calculate TCFs which can be measured in spectroscopic experiments. The autocorrelation function of x for the fOU process reads in particular

$$c_{xx}(t) := \langle x(t)x(0)\rangle = \langle x^2\rangle E_\alpha(-\eta_\alpha t^\alpha). \tag{17}$$

The "anomalous," nonexponential behavior of the autocorrelation function can be related to memory effects, which are introduced through the fractional derivative in Eq. (10). Using the theory of the generalized Langevin equation,[41,42] one can formally assign a memory function to any TCF whose dynamics is governed by the laws of classical or quantum many-body dynamics. Within this framework we have

$$\partial_t c_{xx}(t) = -\int_0^\infty d\tau \xi(t-\tau) c_{xx}(\tau), \tag{18}$$

where $\xi(.)$ is the memory function which can be rigorously expressed in terms of the dynamical variables describing the microscopic dynamics. A simple interpretation in terms of a physical model is, however, difficult. For a correlation function of the form (17), the memory function can be derived by Laplace transform and one finds a power law behavior[6]

$$\xi_{\mathrm{fOU}}(t) = \frac{\alpha-1}{\Gamma(\alpha)\tau^2}\left(\frac{t}{\tau}\right)^{\alpha-2}, \quad t>0, \quad 0<\alpha<1, \tag{19}$$

where $\int_0^\infty dt \xi_{\mathrm{fOU}}(t)=0$.

The fOU process may be used as a heuristic model to interpret NMR relaxation data, i.e., rotational diffusion of bond vectors, if one assumes that the latter fluctuate only moderately about their average direction in a molecular-fixed frame. In this case, the dynamical variables in the diffusion process are the Cartesian coordinates x and y of the bond vector in the plane perpendicular to the average direction.[12,14] Assuming an axially symmetric potential for the corresponding motion

$$V(x,y) = \frac{K}{2}(x^2+y^2) \tag{20}$$

the diffusion will be isotropic with respect to x and y and the parameters of the model are the same as in the 1D case. The position correlation function keeps in particular the form (17). Using the fact that the order parameters can be expressed as $S_i^2 = 1-3\langle x_i^2+y_i^2\rangle$ within the above approximation,[13,14] and that $\langle x_i^2+y_i^2\rangle = 2k_BT/K_i$, it follows that

$$S_i^2 = 1 - \frac{6k_BT}{K_i}. \tag{21}$$

The order parameter is thus related to the elasticity or softness of the protein at the position of residue i. Since the rotational TCFs can be described by a fOU process, we refer to our model with the label "fOU."

IV. RESULTS

A. Comparing model and MD data

The analysis of the internal autocorrelation functions $C_{ii}^I(t)$ obtained from MD simulation was performed as follows:

(1) The decay from $t=0$ to $t=1$ ps is considered *instantaneous* and a correspondingly modified version of model (6) is fitted to the simulated TCFs in the time interval $1\ \mathrm{ps} < t < 1000\ \mathrm{ps}$

$$C_{ii}^I(t) = S_i^2 + (S_{i,f}^2 - S_i^2)E_{\alpha_i}(-[t/\tau_i]^{\alpha_i}). \tag{22}$$

For comparison the simulated TCFs have been fitted in the same time interval using the extended MF approach[43]

$$C_{ii}^I(t) = S_i^2 + (S_{i,f}^2 - S_i^2)\exp(-t/\tau_{\mathrm{MF},i}). \tag{23}$$

In both models $S_{i,f}^2 = C_{ii,\mathrm{MD}}^I(1\ \mathrm{ps})$ are to be considered as given order parameters for the fast motions, which are not explicitly accounted for, and α_i, τ_i, and $\tau_{\mathrm{MF},i}$ are adjustable parameters. The values for S_i^2 are either extracted from the MD simulation or are considered as adjustable parameters as well.

(2) Model (6) is fitted to the simulated TCFs over the whole time scale $0\ \mathrm{ns} \le t \le 1\ \mathrm{ns}$, describing an *average* decay in the oscillatory initial regime between 0 and 1 ps. Again, S_i^2 is either taken from MD simulation or treated as an adjustable parameter, together with α_i and τ_i.

Figure 1 shows the internal correlation functions for a few selected residues (dots), together with the fits of models (22) and (23) for $1\ \mathrm{ps} \le t \le 1000\ \mathrm{ps}$, treating S_i^2 as a fit parameter (solid lines). In the upper right insets we show the fast initial decay of the simulated TCFs. The log-log plot clearly displays systematic deviations of the TCFs from an exponential form, which is quantified by the α parameter in the fOU model and by the corresponding distribution of relaxation rates given in the lower left insets. The MF approach could be in principle improved by introducing a further exponential component, but the MD correlation functions do not specifically suggest the existence of two or more well separated relaxation processes. Figure 2 demonstrates that model (6) is able to account even reasonably well for the steep initial decay of the simulated TCFs for very short time lags ($0\ \mathrm{ps} \le t < 1\ \mathrm{ps}$), leaving out the oscillations the model cannot account for by construction. As for the fits displayed in Fig. 1, S_i^2 was treated as an adjustable parameter.

Figures 3 and 4 show the fitted parameters resulting from the fOU models (6) and (22), where S_i^2 is either an adjustable or a fixed parameter obtained from MD simulation. For comparison we also present the results obtained with the MF approach (23). In the latter case the fit of the TCFs has been carried out only for the reduced time window $1\ \mathrm{ps} < t < 1000\ \mathrm{ps}$. The results show that passing from the full to the reduced time window leads to values of α closer to one—expressing a more exponential character of the TCFs—and an increase of the time scale parameters by approximately two orders of magnitude which thus become closer to those obtained from the MF approach. The deviation of the TCFs from an exponential is nevertheless still substantial in almost the whole protein backbone.

B. Predicting NMR relaxation rates from simulation

So far we have demonstrated that expressions (6) and (22) fit well the rotational correlation functions of the NH vectors obtained by MD simulations and we have also shown that it can be related to a physical model, as well as to the concept of memory functions. In order to further exploit the capabilities of our model, we applied it to the calculation of NMR relaxation rates from an MD simulation of lysozyme in

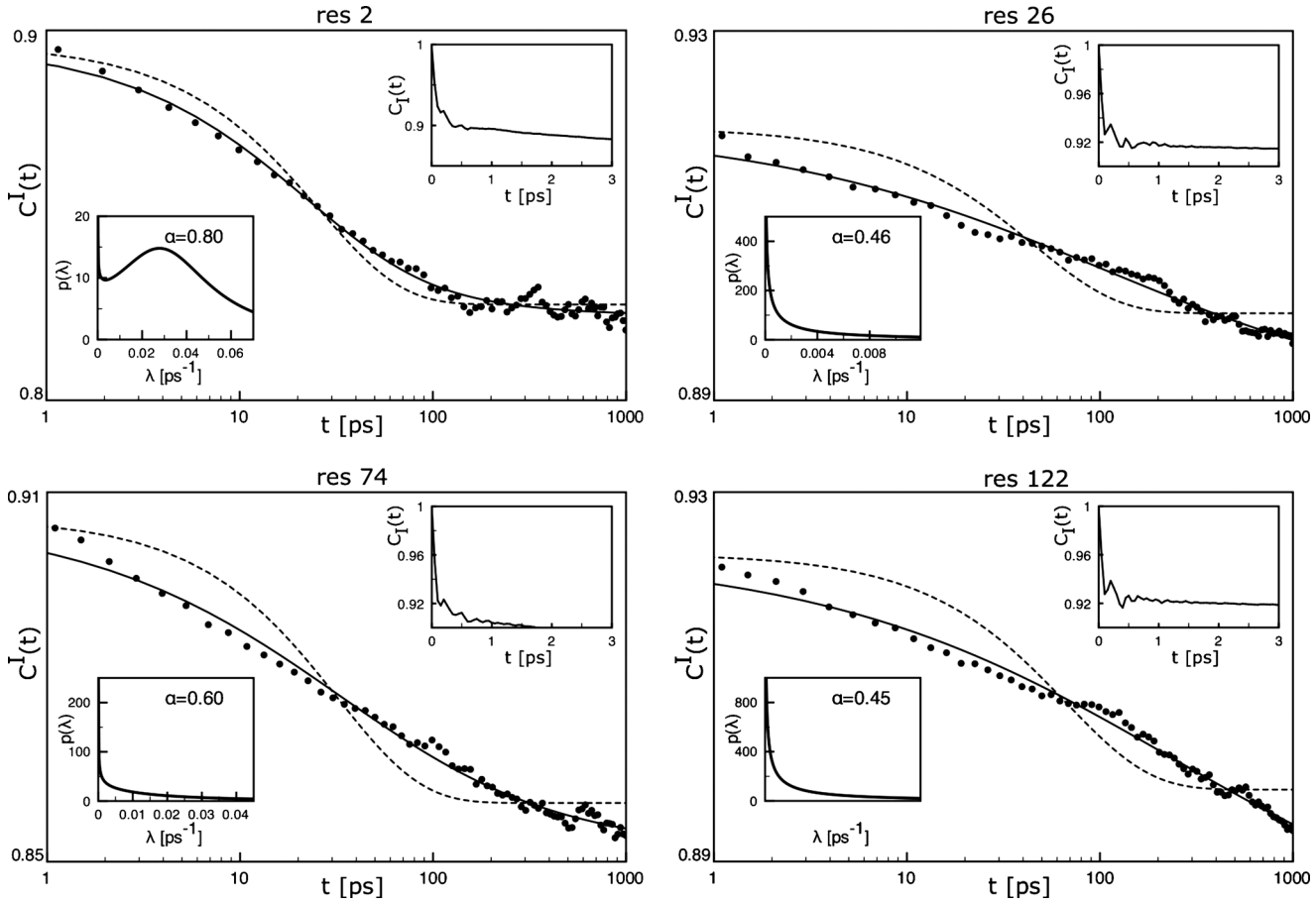

FIG. 1. Internal correlation functions $C_{ii}^{I}(t)$ for selected residues (Val 2, Gly 26, Asn 74, Ala122) computed from MD simulation (dots) together with the fits of model (22) (solid line) and the fit of the corresponding MF representation (23) (short dashes). Both fits are performed for time lags from 1 to 1000 ps. Within each panel the top-right inset shows a zoom on the first few picoseconds of the TCF and the bottom-left inset shows the distribution of relaxation rates according to Eq. (9).

solution and compared the results with experimental data.[15] Using Eq. (6) and the factorization $C_{ii}(t)=C^{G}(t)\cdot C_{ii}^{I}(t)$, where

$$C^{G}(t)=\exp(-t/\tau_0) \tag{24}$$

and τ_0 is the characteristic time scale for the global rotation, it is possible to derive an analytical expression for the spectral densities.[9] To accommodate both versions (6) and (22) of the fOU model and the MF approach (23) (set $\alpha_i=1$ in this case), we write

$$J_{ii}(\omega)=\frac{S_i^2\tau_0}{1+(\omega\tau_0)^2}+(S_{i,f}^2-S_i^2)\times\frac{1}{\gamma}\frac{(\gamma\tau_i)^{\alpha_i}\cos\beta+\cos[\beta(1-\alpha_i)]}{(\gamma\tau_i)^{\alpha_i}+(\gamma\tau_i)^{-\alpha_i}+2\cos\beta\alpha_i}, \tag{25}$$

where $\cos\beta=(\tau_0\gamma)^{-1}$, $\sin\beta=\omega/\gamma$, $\gamma=(\tau_0^{-2}+\omega^2)^{1/2}$, and $S_{i,f}=1$ for the original model (6). For τ_0 we used the value previously determined from NMR relaxation measurements.[15]

To compute NMR relaxation rates from the MD simulation we used both variants (6) and (22) of the fOU model as well as the MF approach (23), in the respective time intervals, where S_i^2 were either treated as a fit parameters or fixed to the respective values computed from the MD trajectory. The results are shown in Figs. 5 and 6. Inspection of η_{NH}, R_1, and R_2 as a function of the residue number shows that our approach yields overall satisfactory agreement with experimental data for both fitting methods used. Both estimations give very similar results for R_1 and R_2 (top and middle panels of Figs. 5 and 6), although the estimates for η_{NH} show somewhat larger differences in some regions of the protein. Only minor differences are observed for the η_{NH} rates of residues 100–105 if S_i^2 fixed to the values obtained from MD simulation, for which the fOU model seems to give a better estimation than the MF approach. To have a better appreciation of the prediction capability of fOU model with respect to MF it would be interesting to increase the number of observables, for example by changing the strength of the magnetic field and thus the Larmor frequencies. Nevertheless, the most important point to keep in mind here is that the fOU model is able to reproduce the experimental data with an accuracy similar to the one provided by the MF approach.

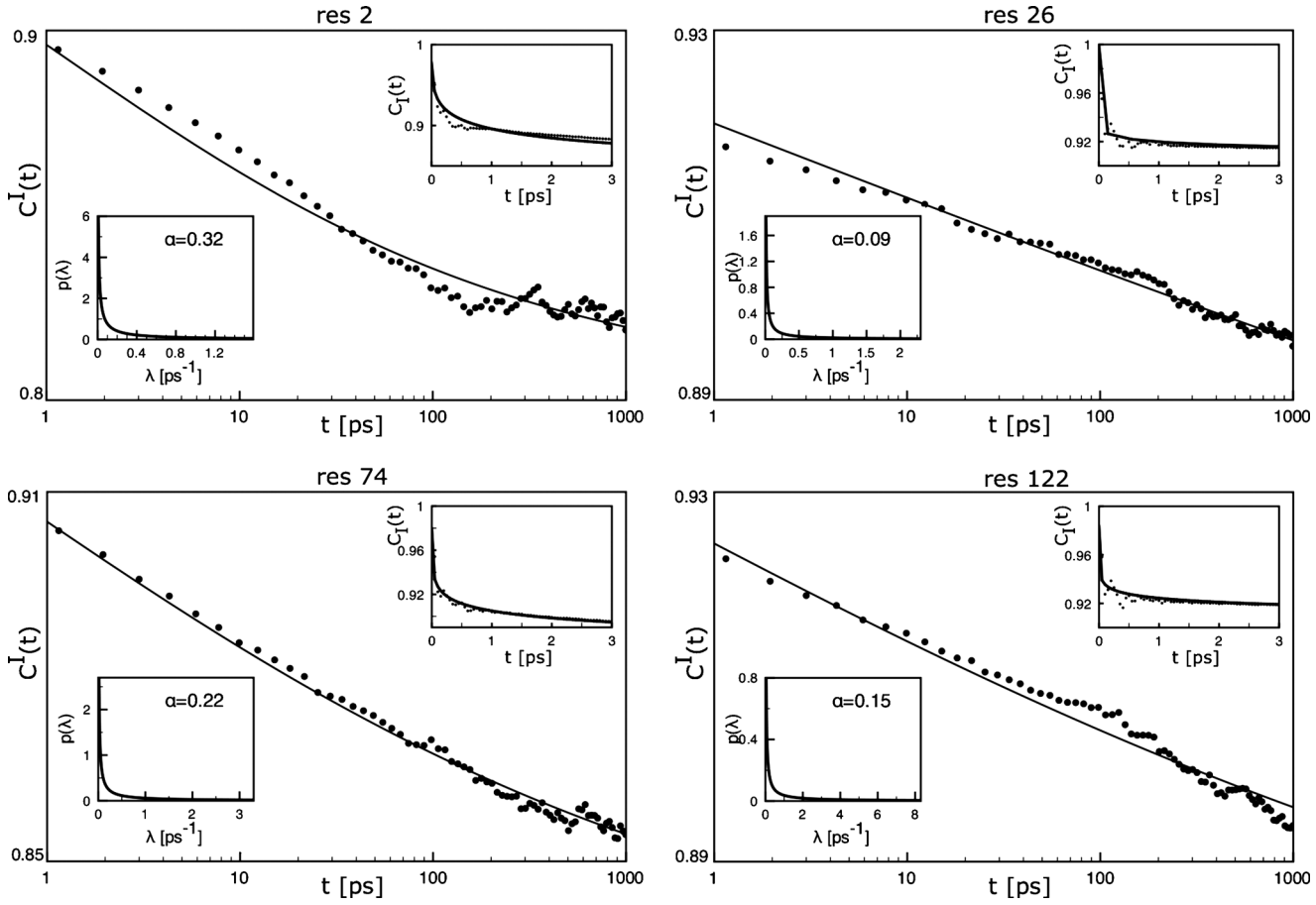

FIG. 2. The simulated internal correlation functions $C_{ii}^{I}(t)$ selected in Fig. 1 (dots) together with the fits of model (6) for 0 ps $\leq t \leq$ 1000 ps (solid line). The upper right inset in each panel shows here a zoom onto the first few picoseconds of the respective TCF (dots) together the fit of model (6) (solid lines) and the bottom-left inset the corresponding distributions of relaxation rates according to Eq. (9).

In addition, our model offers a more realistic picture of internal protein dynamics by introducing a *distribution* of relaxation times/rates. Indeed, the good agreement between the correlation functions computed from MD simulation and their representations by stretched ML functions in the time interval 0 ps $< t <$ 1000 ps, on one hand, and the agreement between back-calculated and experimentally measured relaxation rates, on the other hand, suggests that our model is able to account for the multiscale character of internal protein dynamics. Interestingly, it does so without introducing an arbitrary separation between very fast (subpicosecond) and slower (picosecond-nanosecond) motions, and with no need for an additional parameter accounting for the plateau value of the faster decay. We remark that the prediction of relaxation rates based on a MF approach with two exponential functions does not improve the agreement with the experimental results (data not shown).

As a final point we discuss the relation between the correlation time $\tau_{\mathrm{MF},i}$ of MF correlation function and the correlation time τ_i of fOU model. At low frequencies, $\omega \ll 1/\tau_0$, the spectral densities are dominated by the overall tumbling of the protein. Therefore the two approximate spectral density functions should obey the condition $J_{ii}^{\mathrm{MF}}(0) \approx J_{ii}^{\mathrm{fOU}}(0)$. Equating both values and using that

$$J_{ii}^{\mathrm{fOU}}(0) = S_i^2\tau_0 + (S_{i,f}^2 - S_i^2)\frac{\tau_i\left(\frac{\tau_i}{\tau_0}\right)^{\alpha_i - 1}}{1 + \left(\frac{\tau_i}{\tau_0}\right)^{\alpha_i}}, \tag{26}$$

$$J_{ii}^{\mathrm{MF}}(0) = S_i^2\tau_0 + (S_{i,f}^2 - S_i^2)\frac{\tau_{\mathrm{MF},i}}{1 + \frac{\tau_{\mathrm{MF},i}}{\tau_0}} \tag{27}$$

one obtains a relationship between the MF relaxation time $\tau_{\mathrm{MF},i}$ and the scaling and shape parameters τ_i and α_i of the fOU model

$$\tau_{\mathrm{MF},i} = \tau_i(\tau_i/\tau_0)^{\alpha_i - 1}, \quad 0 < \alpha_i \leq 1. \tag{28}$$

Inserting the fitted parameters α_i and τ_i in the above expression, we obtain values for $\tau_{\mathrm{MF},i}$ in the range between 50 and 1000 ps, which are of the same order as those found by Buck *et al.*[15] using the MF approach. We remark that $\tau_{\mathrm{MF},i}$ is *the* time scale for the internal dynamics of the respective NH vector in the MF approach, whereas the τ_i is the inverse of the median of distribution of relaxation rates.[9] Only for an exponential function the two definitions coincide.

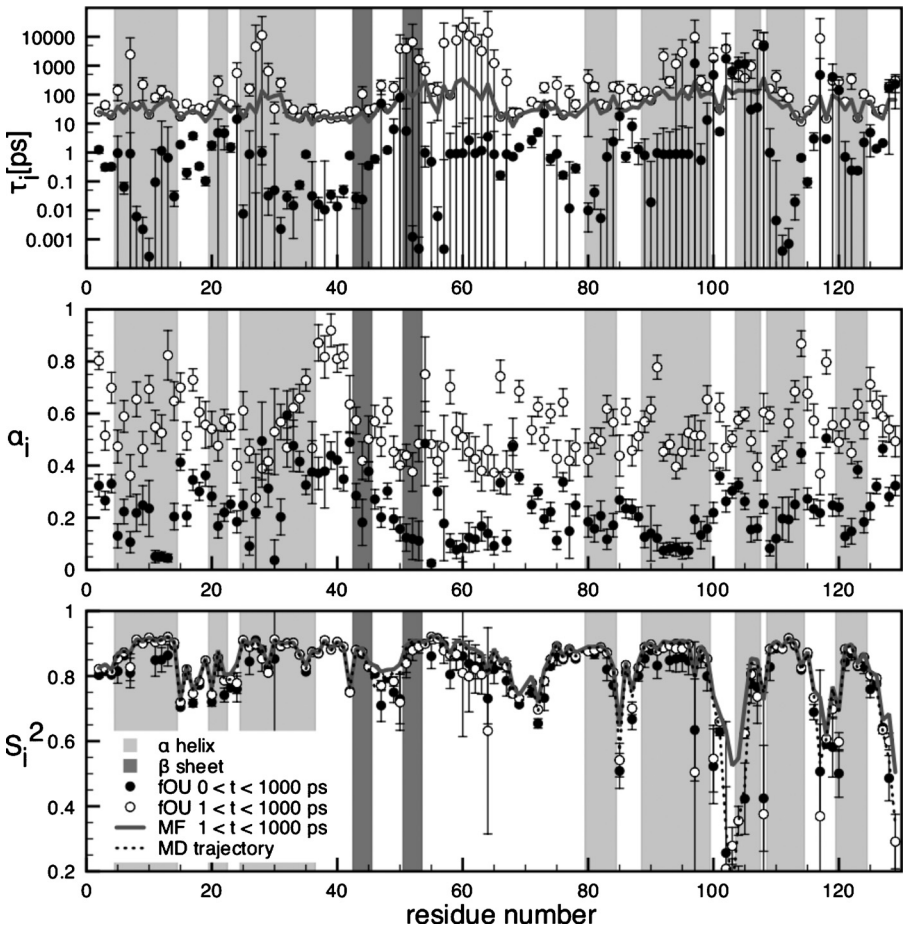

FIG. 3. The fit parameters α_i, τ_i, and S_i^2 corresponding to models (6) (filled circles) and (22) (open circles), together with the fit parameters τ_i and S_i^2 corresponding to the MF approach (gray line). The parameters are shown as a function of the residue number, i. The fits of model (6) have been performed for $0\ \text{ps} \leq t \leq 1000\ \text{ps}$ and those of model (22) and the MF expression (23) for $1\ \text{ps} \leq t \leq 1000\ \text{ps}$. In the bottom panel we show for comparison the values for S_i^2 obtained from MD simulation (short dashed line). The light gray and dark gray stripes indicate α-helices and β-sheets, respectively.

V. CONCLUSIONS

Our results show that the model of fractional Brownian dynamics in a harmonic potential affords a practical way of modeling the internal time autocorrelation functions relevant to NMR relaxation. This approach accounts for the existence of a continuous spectrum of time scales in the internal dynamics of proteins, keeping the number of model parameters at a strict minimum. The fOU model provides estimations of the relaxation rates η_{NH}, R_1, and R_2 which are of similar quality as those obtained from the (extended) MF approach, yielding at the same time a better representation of the relevant reorientational TCFs, even if the steep decay for short times is considered. It is in particular a clear alternative

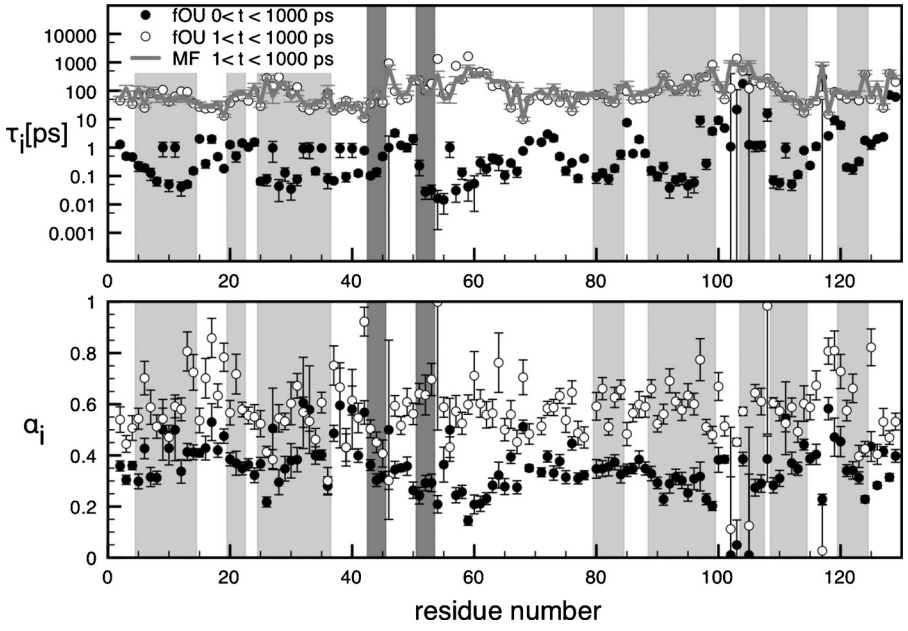

FIG. 4. As Fig. 3, but with S_i^2 taken from MD simulation.

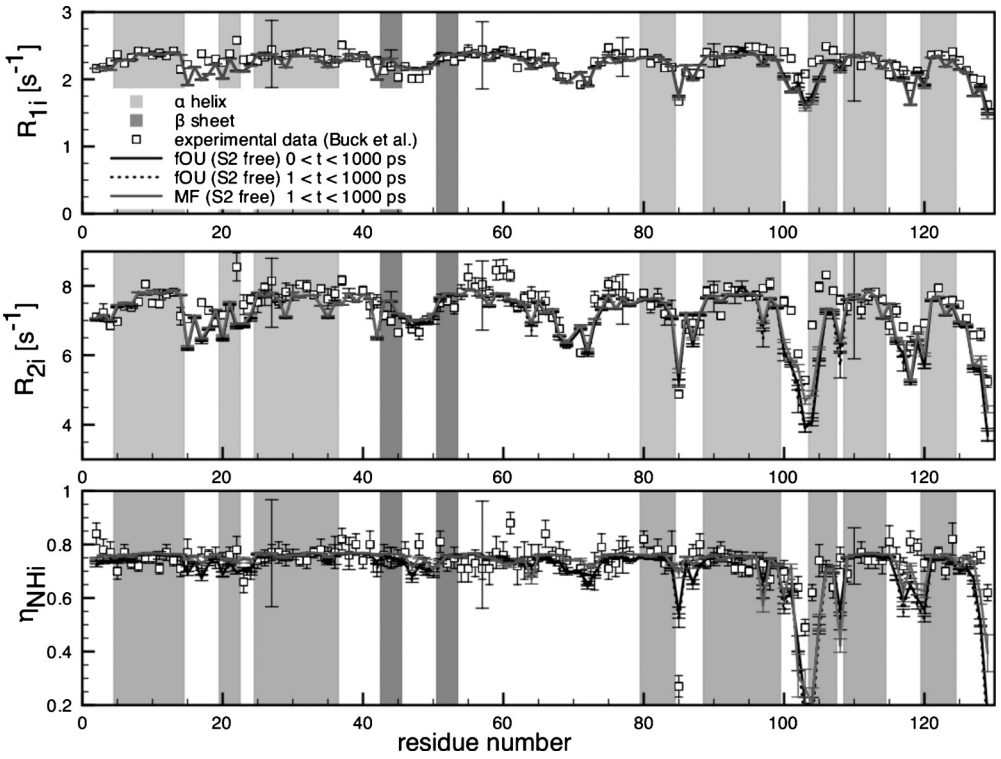

FIG. 5. Estimation of R_1, R_2, and η_{NH} from MD simulation using the parameters obtained from the fits based on the fOU models (6) and (22) and on the MF approach (23). Here S_i^2 are considered as fit parameters.

to accounting for the nonexponential form of the TCFs by increasing the number of exponential components in the MF approach, since this method would not only require the introduction of two additional adjustable parameters per exponential function, but would rapidly also lead to an unstable fitting procedure. Here the fOU model offers an affordable way of capturing multiscale relaxation processes in protein dynamics through a distribution of relaxation rates which can be described by only two parameters. Work on the direct application to simulation data and on applications with an anisotropic extension of the harmonic potential (20) is in progress.

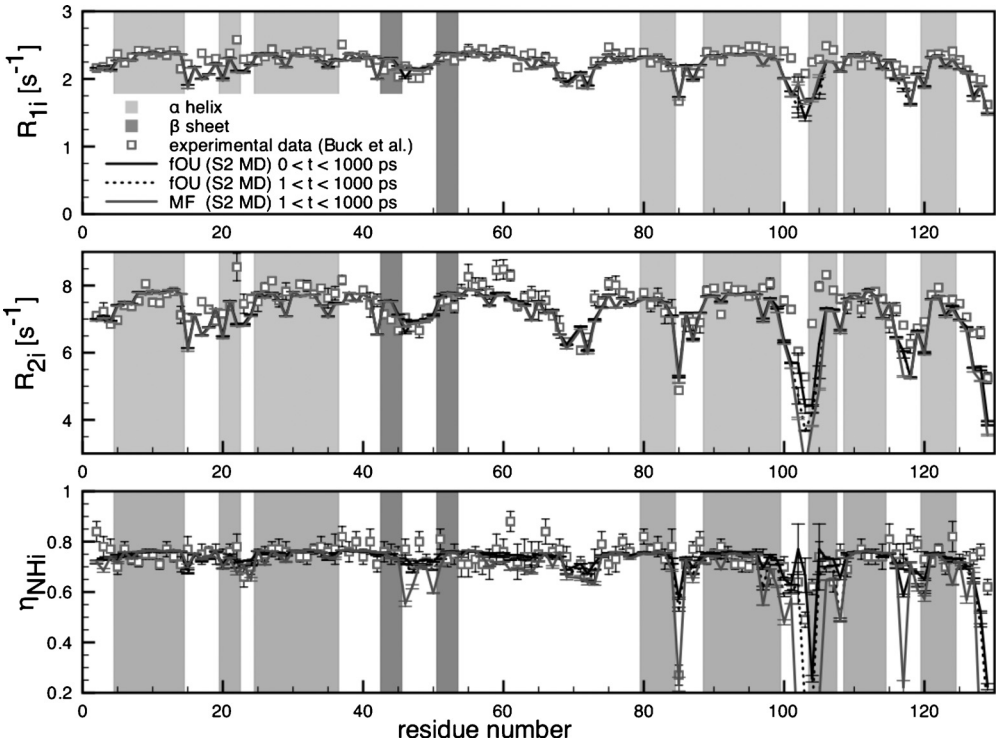

FIG. 6. As for Fig. 5, but with S_i^2 taken from MD simulation.

ACKNOWLEDGMENTS

We wish to thank Paolo Calligari for his support concerning the MD simulation. V.C. acknowledges financial support by the Agence Nationale de la Recherche (Contract No. ANR-06-CIS6-012-01).

[1] A. Redfield, IBM J. Res. Dev. **1**, 19 (1957).
[2] D. M. Korzhnev, M. Billeter, A. S. Arseniev, and V. Y. Orekhov, Prog. Nucl. Magn. Reson. Spectrosc. **38**, 197 (2001).
[3] G. Lipari and A. Szabo, J. Am. Chem. Soc. **104**, 4546 (1982).
[4] W. Glöckle and T. Nonnenmacher, Biophys. J. **68**, 46 (1995).
[5] H. Yang, G. Luo, P. Karnchanaphanurach, T. Louie, I. Rech, S. Cova, L. Xun, and X. Xie, Science **302**, 262 (2003).
[6] G. Kneller and K. Hinsen, J. Chem. Phys. **121**, 10278 (2004).
[7] G. Kneller, Phys. Chem. Chem. Phys. **7**, 2641 (2005).
[8] V. Calandrini, V. Hamon, K. Hinsen, P. Calligari, M.-C. Bellissent-Funel, and G. Kneller, Chem. Phys. **345**, 289 (2008).
[9] V. Calandrini, D. Abergel, and G. Kneller, J. Chem. Phys. **128**, 145102 (2008).
[10] G. Kneller and V. Calandrini, Biochim. Biophys. Acta **1804**, 56 (2010).
[11] R. Metzler and J. Klafter, Phys. Rep. **339**, 1 (2000).
[12] V. Calandrini and G. Kneller, J. Chem. Phys. **128**, 065102 (2008).
[13] D. Abergel and G. Bodenhausen, J. Chem. Phys. **121**, 761 (2004).
[14] D. Abergel and G. Bodenhausen, J. Chem. Phys. **123**, 204901 (2005).
[15] M. Buck, J. Boyd, C. Redfield, D. MacKenzie, D. Jeenes, D. Archer, and C. Dobson, Biochemistry **34**, 4041 (1995).
[16] M. Vaney, S. Maignan, M. RiesKautt, and A. Ducruix, Acta Crystallogr., Sect. D: Biol. Crystallogr. **52**, 505 (1996).
[17] J. C. Phillips, R. Braun, W. Wang, J. Gumbart, E. Tajkhorshid, E. Villa, C. Chipot, R. D. Skeel, L. Kalé, and K. Schulten, J. Comput. Chem. **26**, 1781 (2005).
[18] V. Hornak, R. Abel, A. Okur, B. Strockbine, A. Roitberg, and C. Simmerling, Proteins **65**, 712 (2006).
[19] H. Berendsen, J. Grigera, and T. Straatsma, J. Phys. Chem. **91**, 6269 (1987).
[20] T. Darden, D. York, and L. Pedersen, J. Chem. Phys. **98**, 10089 (1993).
[21] J. A. Izaguirre, D. P. Catarello, J. M. Wozniak, and R. D. Skeel, J. Chem. Phys. **114**, 2090 (2001).
[22] S. Nosé, Prog. Theor. Phys. **103**, 1 (1991).
[23] G. Kneller, Mol. Simul. **7**, 113 (1991).
[24] G. Kneller, J. Comput. Chem. **26**, 1660 (2005).
[25] B. Halle, J. Chem. Phys. **131**, 224507 (2009).
[26] E. Meirovitch, Y. Shapiro, A. Polimeno, and J. H. Freed, Prog. Nucl. Magn. Reson. Spectrosc. **56**, 360 (2010).
[27] T. Róg, K. Murzyn, K. Hinsen, and G. Kneller, J. Comput. Chem. **24**, 657 (2003).
[28] M. Abramowitz and I. Stegun, *Handbook of Mathematical Functions* (Dover, New York, 1972).
[29] A. Erdélyi, W. Magnus, F. Oberhettinger, and F. Tricomi, *Higher Transcendental Functions* (McGraw Hill, New York, 1955).
[30] A. Kilbas, H. Srivastava, and J. Trujillo, *North Holland Mathematics Studies* (Elsevier, New York, 2006), Vol. 204.
[31] R. Metzler and J. Klafter, J. Phys. A **37**, R161 (2004).
[32] M. Wang and G. Uhlenbeck, Phys. Rev. **93**, 249 (1945).
[33] C. Gardiner, *Handbook of Stochastic Methods*, Springer Series in Synergetics, 2nd ed. (Springer, Berlin, 1985).
[34] N. van Kampen, *Stochastic Processes in Physics and Chemistry* (North Holland, Amsterdam, 1992).
[35] H. Risken, *The Fokker–Planck Equation*, Springer Series in Synergetics, 2nd ed. (Springer, Berlin, 1996).
[36] G. Zaccai, Science **288**, 1604 (2000).
[37] S. Kou and X. Xie, Phys. Rev. Lett. **93**, 180603 (2004).
[38] H. Frauenfelder, F. Parak, and R. Young, Annu. Rev. Biophys. Biophys. Chem. **17**, 451 (1988).
[39] K. Henzler-Wildman and D. Kern, Nature (London) **450**, 964 (2007).
[40] K. Oldham and J. Spanier, *The Fractional Calculus* (Academic, New York, 1974).
[41] R. Zwanzig, *Statistical Mechanics of Irreversibility*, Lectures in Theoretical Physics (Wiley-Interscience, New York, 1961), pp. 106–141.
[42] R. Zwanzig, *Nonequilibrium Statistical Mechanics* (Oxford University Press, New York, 2001).
[43] G. M. Clore, A. Szabo, A. Bax, L. E. Kay, P. C. Driscoll, and A. M. Gronenborn, J. Am. Chem. Soc. **112**, 4989 (1990).